

Predictive study on Mechanical strength of Lightweight concrete using MRA and ANN

R. Pranamika¹, Dr. M. Senthil Pandian², Prof.K. Karthikeyan³

¹M. Tech (IInd Year Structural Engineering) School of Civil Engineering, VIT, Chennai, India

²Dr. M. Senthil Pandian [Assistant Professor (Sr.)] SCE, VIT Chennai, India

³Prof.K. Karthikeyan [Assistant Professor (Sr.)] SCE, VIT Chennai, India

¹Email: pranamikaramachamdran@gmail.com

²Email: senthilpandian_06@yachoo.co.in

³Email: kothandapanikarthikeyan@gmail.com

Article History: Received: 10 January 2021; Revised: 12 February 2021; Accepted: 27 March 2021; Published online: 28 April 2021

Abstract: The lightweight concrete is preferred over regular density concrete as it which reduces the dead load of the structure due to its lower density. The reduction in dead load of the structure, resulting in a considerable decrease in the size of structural elements and reinforcements; thereby, the building's cost can be reduced. The lightweight concrete is achieved through natural lightweight aggregates, artificial lightweight aggregates, coconut shells, oil palm shells, aeration in concrete, etc. The mechanical properties like compressive strength, tensile strength, density depend upon lightweight aggregate, fine aggregate, super-plasticizer, cement content, water-cement ratio, etc. The mechanical properties can also be predicted using artificial intelligence from the existing data. This research aims to predict lightweight concrete's mechanical properties using MRA and ANN accurately.

Keywords: artificial neural network; compressive strength; lightweight aggregate concrete

1. Introduction:

Lightweight aggregate concrete (LWAC) is a kind of concrete which has a low unit weight when balanced to that of normal weight aggregate concrete (NWAC). The low mass density of it has one of the big favors correlated with truncated self-weight of structures & is also enacted in long-span bridges and high-rise buildings. Also, the, structural LWAC, with a strength that is akin to NWAC, enables the limiting of construction outlay as it entails less reinforcement, minuscule assisting deck members, beams, & piers, & less earth tremor ruinous, the viable ease of LWAC is the haulage cost stockpile achieved by outstrip the upheave skillfulness in the construction field and lowering shipping cost, compared to conventional NWAC products.

LWAC has the same concrete components as conventional NWAC with a partial or complete substitute of normal weight aggregate (NWA) with lightweight aggregate (LWA). The LWAs have an inherently great porosity, contributing in low density, low strength, and deformable particles. LWAs generally has a density lower than 1920 kg/m³. A lower density of LWAC can be achieved by using a heftier lump of porous LWA, trickle-down abject mechanical performance. Compressive strength of LWAC relay on not only the content of LWAs, but also on other factors. Hence, these experimental studies shows that the properties & amount of LWAs influenced the mechanical behavior of LWAC. the mix proportions of LWAC are also the key parameters incite the capacity of LWAC, such as water-to-cement ratio (w/c) & mass of aggregate, water, & binders including cement, fly ash, & silica fume. The intricate relationship between concrete constituents & properties of cement-based construction materials, researchers have employed artificial neural networks (ANN). In the field of construction materials, ANN methods were applied for creating concrete properties, including mechanical, fluidity, &

durability in concrete components-related information as input parameters. This study gives a prediction model created on ANN and MRA based on mechanical characteristics of LWAC, which enable us to produce high-quality LWAC, satisfying the target performance.

Detailed & extensive data on the mix proportions & the mechanical behavior of LWAC are taken from literature. The vast amount of data allows to enhance the reliability and accuracy of the prediction model. The prediction model is evaluated and compared to the results obtained from the commonly used statistical models.

2. Prediction Modeling and Testing:

Depending on the input parameter & target values, the output was effectuated through MRA and ANN, output values were equated with target (actual) values. Types of fibers and its respective literature source are presented in Table 1. Active compressive strength (3 days) data set has 64 columns and 3916 rows (64×3916) of input data and 1 column and 3916 rows (1×3916) of target data. Active compressive strength (7 days) data set has 64 columns and 3916 rows (64×3916) of input data and 1 column and 3916 rows (1×3916) of target data. Active compressive strength (14 days) data set has 64 columns and 3916 rows (64×3916) of input data and 1 column and 3916 rows (1×3916) of target data. Active compressive strength (28 days) data set has 64 columns and 3916 rows (64×3916) of input data and 1 column and 3916 rows (1×3916) of target data. Active split tensile strength data set has 5 columns and 1328 rows (5×1328) of input data and 1 column and 119 rows (1×1322) of target data. Active Density data set has 64 columns and 2872 rows (64×2872) of input data and 1 column and 2872 rows (1×2872) of target data. Target data for density, compressive strength and split tensile strength were used in both the MRA and ANN model as separate target in this study.

Table 1: Range of parameters in data base for prediction model

S. No.	Type	Type of Material	Material	Unit	Content Range
1.	<i>INPUT</i>	<i>OTHER PARAMETERS</i>	Cement	Kg/m ³	0 to 815
2.			NWA	Kg/m ³	0 to 1296
3.			Fine aggregate (Natural Sand)	Kg/m ³	0 to 1600
4.			Fine aggregate (M-sand)	Kg/m ³	0 to 659.5
5.			Water	Kg/m ³	37.5 to 323
6.			W/B ratio	-	0.1 to 2.18
7.			GGBS	Kg/m ³	0 to 180
8.			Phosphogypsum	Kg/m ³	38.2
9.			Crushed Ceramic	Kg/m ³	0 to 45
10.			Fly ash cenosphere	Kg/m ³	0 to 203
11.			Recycled aggregate	Kg/m ³	0 to 334.74
12.			Self-Compacting Agent	%	0 to 1.2
13.			Pulverized fuel ash	Kg/m ³	0 to 138
14.			Nano palm oil fuel ash	Kg/m ³	0 to 150

15.		Silica fume	Kg/m ³	0 to 180
16.		Lime stone powder	Kg/m ³	0 to 150
17.		Steel fiber	Kg/m ³	0 to 39
18.		Carbon fiber	%	0 to 1.5
19.		Acrylic polymer	%	0 to 10
20.		Long Polypropylene fibre	Kg/m ³	0 to 12
21.		Long Polyolefin fibre	%	0 to 9
22.		Short Polyolefin fibre	%	0 to 2
23.		Poly vinyl Chloride Granules	Kg/m ³	0 to 135
24.		Metakaolin	Kg/m ³	0 to 102
25.		Mineral Admixture	Kg/m ³	0 to 200
26.		Rice husk ash	Kg/m ³	0 to 112.5
27.		Fly Ash	Kg/m ³	0 to 300
28.		Air entraining agent	Kg/m ³	0 to 2.73
29.		Alcofine	Kg/m ³	0 to 59.1
30.		Glass powder	Kg/m ³	0 to 1610
31.		Egg Shell powder	Kg/m ³	0 to 90
32.		Viscosity modifier	%	0 to 1.65
33.		Superplasticizer	Kg/m ³	0 to 30.6
34.		HCL	%	0 to 5
35.		MgSO4	%	0 to 5
36.		NaCl	%	0 to 5
37.		Temperature of Curing	°C	18 to 1000
38.	LIGHT WEIGHT AGGREGATES	Cinder	Kg/m ³	0 to 1119
39.		LECA	Kg/m ³	0 to 1119
40.		Recycled LECA	Kg/m ³	0 to 350
41.		Lava or tuff LWA	Kg/m ³	0 to 1060
42.		Expanded Clay	Kg/m ³	0 to 1152
43.		Bagacina Aggregate	Kg/m ³	0 to 946
44.		Flashag	Kg/m ³	0 to 766
45.		Lyttag	Kg/m ³	0 to 1270
46.		Litcon	Kg/m ³	0 to 647
47.		Crushed Animal Bone	Kg/m ³	0 to 421
48.		Apricot Shell	Kg/m ³	0 to 421

49.		Argex	Kg/m ³	0 to 592
50.		Car fluff	Kg/m ³	0 to 468
51.		Coal Gangue Aggregate	Kg/m ³	0 to 1005
52.		Arlita	Kg/m ³	0 to 643
53.		Procelinite	Kg/m ³	0 to 510
54.		Paraffin impregnated LA	Kg/m ³	0 to 488
55.		PUR Foam	Kg/m ³	0 to 20.1
56.		Expanded Shale	Kg/m ³	0 to 879
57.		Expanded Polystyrene (EPS)	Kg/m ³	0 to 1920
58.		Sintered Fly ash Aggregate	Kg/m ³	0 to 975
59.		Styrofoam	Kg/m ³	0 to 992
60.		Expanded waste glass	Kg/m ³	0 to 580
61.		Scoria	Kg/m ³	0 to 1290
62.		Waste Plastic	Kg/m ³	0 to 246
63.		Furnace Bottom ash	Kg/m ³	0 to 1835
64.		Zeolite	Kg/m ³	0 to 550
65.		Diatomite	Kg/m ³	0 to 607
66.		Pumice	Kg/m ³	0 to 1000
67.		Rubber Powder	Kg/m ³	0 to 88.9
68.		Autoclaved Aerated Concrete	Kg/m ³	0 to 389
69.		Expanded Perlite Aggregate	Kg/m ³	0 to 319
70.		Oil Palm Boiler Clinker	Kg/m ³	0 to 377
71.		Cold Bonded Pelletized	Kg/m ³	0 to 634
72.		Palm Kernel Shells	Kg/m ³	0 to 576.9

2.1 Artificial Neural Network (ANN):

Prediction model done is through MATLAB with two hidden layers, (10 and 15 neurons) in every hidden layer & one output layer with dependent variable as density, compressive strength and split tensile strength. Along with all the data, approximately 70%, 15%, &15% has been scrutinized for training, testing, & validation. The Levenberg– Marquardt (LM) algorithm is utilized for training due to its robustness & speed. Layered feed-forward networks have been practiced in this algorithm, in which the neurons are grouped in layers. Here, signals are sent forward & errors are propagated backwards.

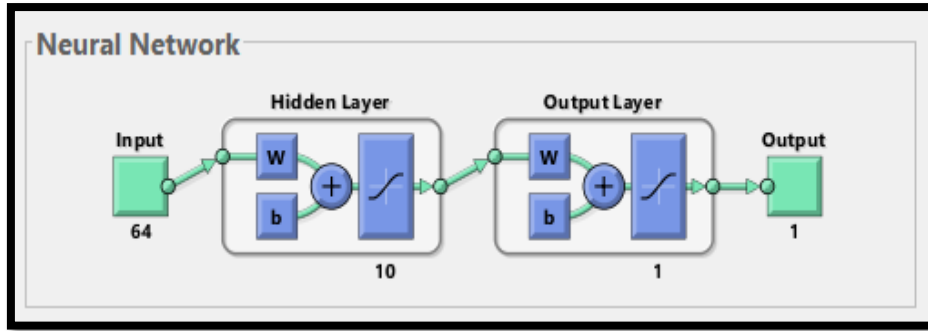


Figure 1: Neural Network with 10 neurons

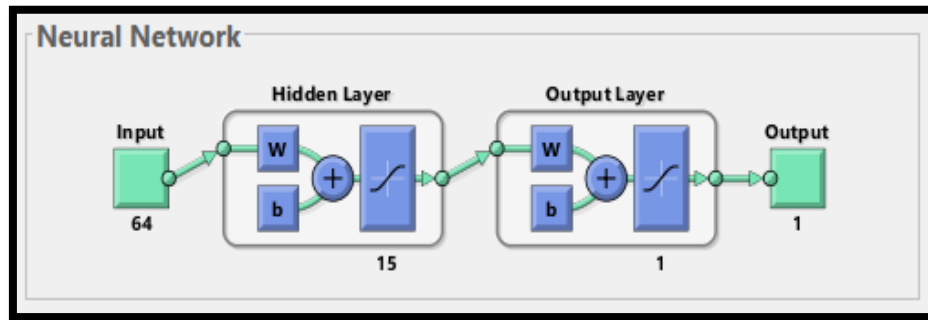


Figure 2: Neural Network with 15 neurons

2.2 Multiple Regression Analysis (MRA):

In this study, the linear-type MRA modeling is done using MS excel. Coefficients of regression are evaluated by considering 95% confidence level, the error tolerance level is restricted to utmost of 5%. For a given input variable, the probability value is considered to be significant, only if it is less than 0.05. *From MRA, the backing coefficients presented in Table () were found and substituted in linear multiple regression equation (equation (1)):

$$O = I + C_1X_1 + C_2X_2 + C_3X_3 + \dots + C_nX_n \tag{1}$$

2.3 Statistical Test:

The prediction model is done with MRA and ANN and the analysis is done regression analysis where the coefficient of determination (R^2) where the accuracy is checked with the values which gives us the validation of the model which is being created by various prediction modeling. This coefficient generally checks the difference or the amount of deviation from one value to the other value. Here the coefficient of determination is used for checking the deviation of the predicted value from the original value. The range of the R^2 varies from 0 to 1 (i.e., 0 to 100 %). (R^2) determination is give in equation (2), precision of the predictions of a network was appraised by RMSE difference, between the experimented and the predicted values.

$$R^2 = \frac{\text{Sum of Squares of Residuals}}{\text{Sum of Squares of Predicted Values,}} \tag{2}$$

In this study, the models were prepared to predict the mechanical behavior (mechanical strength) of LWAC based on input parameters, & four methods were used, ANN, MRA, Orange & Anaconda, prediction models are validated R^2 & RMSE & are consolidated in Table.

To determine compressive strength of various days based on the parameter having various types of

inputs, by using ANN and MRA. The validation of the model is made with coefficient of regression (R^2) shown in table 1.

3. Results and Discussion:

Table 2: MRA Coefficients

MRA Coefficients	Coefficients for Compressive strength (3 days)	Coefficients for Compressive strength (7 days)	Coefficients for Compressive strength (14 days)	Coefficients for Compressive strength (28 days)	Coefficients for Density	Coefficients for Split Tensile Strength
I	2.38032	3.55308	6.02121	6.6576	1043.08	-0.619083
C ₁	0.045053	0.058579	0.061135	0.067849	0.949322	0.00593425
C ₂	0.000166	-0.00032	0.000244	0.000154	0.500255	5.64E-05
C ₃	0.000132	-0.00031	-0.00051	-0.00056	0.386419	0.000895789
C ₄	0.032119	0.043997	0.046736	0.051433	-0.212995	0.00305804
C ₅	0.002141	0.002765	0.003566	0.003928	0.561009	0.000648862
C ₆	0.018629	0.020828	0.019795	0.021919	0.107203	0.00259332
C ₇	0.013255	0.017739	0.019545	0.021637	0.25494	0.00135205
C ₈	0.025377	0.01594	0.037992	0.042464	0.550185	0.00253718
C ₉	0.00917	0.012888	0.01388	0.015329	0.363469	0.00207721
C ₁₀	0.007919	0.013115	0.0116	0.012722	0.258853	6.63E-15
C ₁₁	-0.00988	-0.01563	-0.01454	-0.01626	0.00395855	-7.28E-15
C ₁₂	-0.02937	-0.03496	-0.02924	-0.03283	0.121341	-0.00468068
C ₁₃	0.006064	0.002505	-0.00099	-0.00117	0.376568	2.12E-03
C ₁₄	0.005817	0.007737	0.00743	0.008001	8.89E-11	-5.23E-15
C ₁₅	0.005604	0.008271	0.008659	0.009538	4.94E-11	3.79E-15
C ₁₆	0.040866	0.050252	0.052217	0.057977	1.03544	0.00276373
C ₁₇	-0.00842	-0.01376	-0.01343	-0.01419	0.661361	1.76E-03
C ₁₈	-0.0063	-0.0075	-0.00857	-0.00978	-1.08E-10	-2.39E-15
C ₁₉	0.017669	0.027354	0.027243	0.030255	-3.13353	3.60E-15
C ₂₀	0.010056	0.01177	0.014957	0.016641	0.371877	0.000844433
C ₂₁	-0.01258	-0.01673	-0.01927	-0.0214	-0.298007	-0.00113517
C ₂₂	0.010354	0.013947	0.015109	0.016907	0.476244	1.28E-03
C ₂₃	0.003949	-0.00635	0.005952	0.006487	-0.0324178	9.02E-17
C ₂₄	-0.00449	-0.00657	-0.00794	-0.00844	-1.7652	0.00238174
C ₂₅	0.006525	0.007266	0.008882	0.00986	0.829088	0.00166167
C ₂₆	-0.0357	-0.04426	-0.05477	-0.06164	2.29005	0.0042848
C ₂₇	-0.00194	-0.00225	-0.00241	-0.00269	0.197301	1.05E-03
C ₂₈	-0.00329	-0.00521	-0.00759	-0.00847	9.58E-12	-3.47E-05
C ₂₉	-0.02471	-0.03059	-0.0366	-0.04072	-0.863844	-0.00373247
C ₃₀	-0.00098	-0.00287	-0.0026	-0.00291	0.0245589	0.00151616

C ₃₁	-0.01155	-0.01433	-0.01673	-0.01868	-0.529784	-6.72E-03
C ₃₂	0.015648	0.014012	0.02524	0.02778	-8.20E-12	-1.12E-15
C ₃₃	0.013516	0.01802	0.020299	0.022475	-0.528651	-0.00589151
C ₃₄	0.010673	0.012461	0.012505	0.013527	0.445427	0.00112109
C ₃₅	0.005993	0.008256	0.008685	0.009512	0.464691	0.00050896 2
C ₃₆	-0.00744	-0.01019	-0.01192	-0.0129	0.0955172	-0.00049035
C ₃₇	0.005021	0.005633	0.006539	0.007306	0.633706	0.00081739 7
C ₃₈	0.001394	0.001252	0.001796	0.002116	0.404644	0.00105833
C ₃₉	-0.02834	-0.03521	-0.03819	-0.04197	-0.0644694	-0.00108362
C ₄₀	0.85582	0.95742	0.581363	0.622925	-86.6435	0.339186
C ₄₁	0.028164	0.031083	0.031279	0.035099	0.5785	0.00623413
C ₄₂	0.029433	-0.11661	0.065899	0.067589	6.52045	0.00337422
C ₄₃	0.008242	0.010409	0.012887	0.014469	0.312472	0.00201079
C ₄₄	-0.00628	-0.00952	-0.0118	-0.01321	-0.295232	8.22E-02
C ₄₅	-0.0354	-0.04825	-0.05372	-0.06069	2.03E-11	-4.23E-16
C ₄₆	0.006207	0.014797	0.010844	0.012298	1.29311	8.02E-04
C ₄₇	-11.6904	-14.8111	-16.8068	-18.7674	1.68E-11	8.15E-17
C ₄₈	0.094337	0.126536	0.138194	0.153367	0.584081	2.31E-03
C ₄₉	0.074514	0.108618	0.12141	0.134903	0.0322259	8.26E-16
C ₅₀	0.060584	0.067604	0.081497	0.088151	-0.949852	0.0055876
C ₅₁	0.00255	0.003282	0.004305	0.005225	0.278889	0.00052738 1
C ₅₂	0.049276	0.070024	0.082441	0.090823	0.855489	0.0200675
C ₅₃	2.53413	3.9014	4.02435	4.76044	-97.3244	0.0402886
C ₅₄	-1.40316	-1.98531	-2.2921	-2.36887	-355.706	-0.135955
C ₅₅	-0.98352	-1.09846	-1.38175	-1.54683	-0.288068	-0.0052128
C ₅₆	0.520374	2.38635	1.40609	1.2306	-186.678	0.521851
C ₅₇	-55.7382	-76.2212	-87.5386	-97.6039	-3231.89	0
C ₅₈	-0.00287	-0.00118	-0.00351	-0.00467	-1.79762	0
C ₅₉	0.168384	0.205624	0.174972	0.193376	0.575862	0.00099540 4
C ₆₀	0.082083	0.10913	0.118606	0.132048	-9.09E-13	0
C ₆₁	0.032157	0.031562	0.04653	0.056991	0.253914	0.00601884
C ₆₂	0.030874	0.041114	0.044818	0.049362	0.371824	0.00191702
C ₆₃	-0.10382	-0.19761	-0.25577	-0.2869	-30.1543	-0.00072990
C ₆₄	0.022219	-0.33514	0.05833	0.061312	-0.856159	0
C ₆₅	0.010267	0.014832	0.015409	0.017255	0.426899	0.00296507
C ₆₆	0.042164	0.053876	0.056989	0.061443	1.68015	0.0057291
C ₆₇	-1.03437	-1.21501	-0.89835	-1.03408	-22.414	0.339932
C ₆₈	-0.11549	-0.10689	-0.12224	-0.13553	-5.04692	0.00584847
C ₆₉	0.405153	0.773858	0.706565	0.77447	0	0

C ₇₀	1.12059	1.72778	1.77973	1.96687	0	0
C ₇₁	1.29891	1.96554	2.04721	2.26407	0	0
C ₇₂	-0.00884	-0.0103	-0.01242	-0.01389	0.0212851	-0.00289578

Table 2: R² values

Sr. No.	redicted Parameters	MRA		ANN (10 Neurons)		ANN (15 neurons)	
		R ²	RMSE	R ²	RMSE	R ²	RMSE
1.	Compressive strength (3 days)	0.4753	7.9	0.8234	4.59883	0.825	4.58367
2.	Compressive strength (7 days)	0.4878	9.958	0.8009	6.223	0.8292	5.7606
3.	Compressive strength (14 days)	0.4969	10.715	0.8087	6.6396	0.8422	6.0026
4.	Compressive strength (28 days)	0.4969	11.877	0.8326	6.88715	0.8498	7.49254
5.	Density	0.6315	250.599	0.7842	190.9408	0.7955	186.3410
6.	Split tensile strength	0.4076	1.276	0.7241	0.88253	0.7383	0.8834

The prediction of ANN and MRA for compressive strength of 3 days is shown in Fig 1, 2 and 3 where the R² predictions are shown. It has been found out that prediction for MRA is 0.5474, ANN (10 neurons) is 0.854 whereas on the other side for ANN (15 neurons) it is 0.8698. On the basis of these results, we can easily say that ANN (15 neurons) has more accuracy and can be used for prediction model. The efficiency of prediction model is totally depending on the accuracy of the output. In MRA the lower value of coefficient of regression only depicts that there will be more errors occur as compared to ANN model. So, we cannot use MRA model here for prediction of compressive strength of light weight concrete. Only ANN model can be taken into consideration for output.

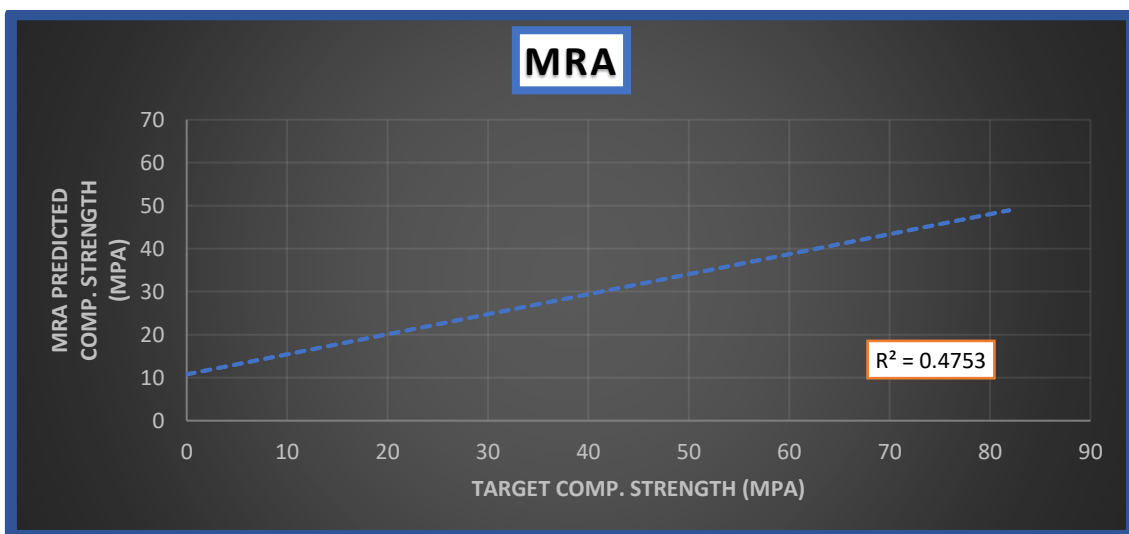


Figure 3: Target vs. MRA (3 days) compressive strength

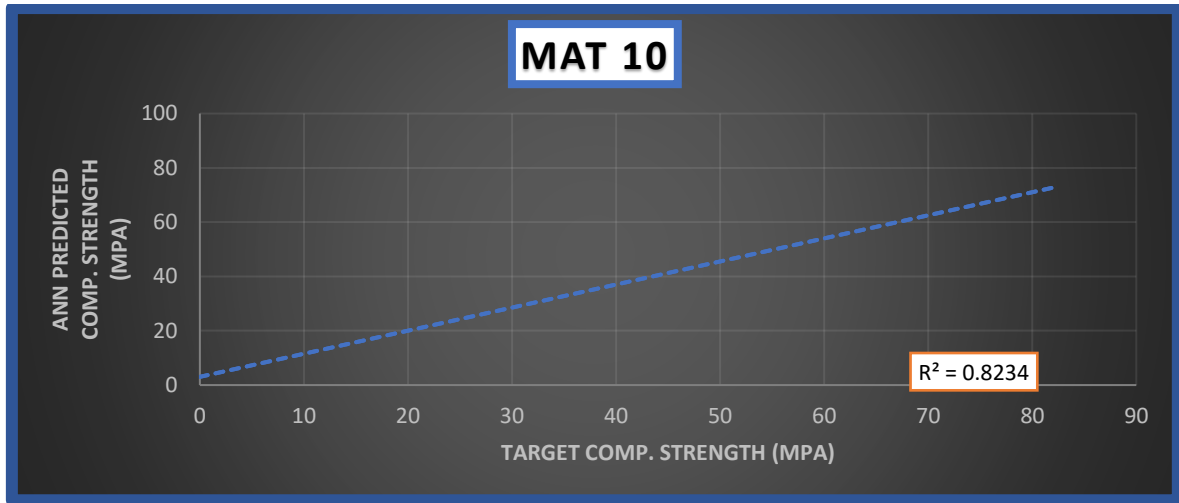


Figure 4: Target vs. ANN (10 neurons) (3 days) compressive strength

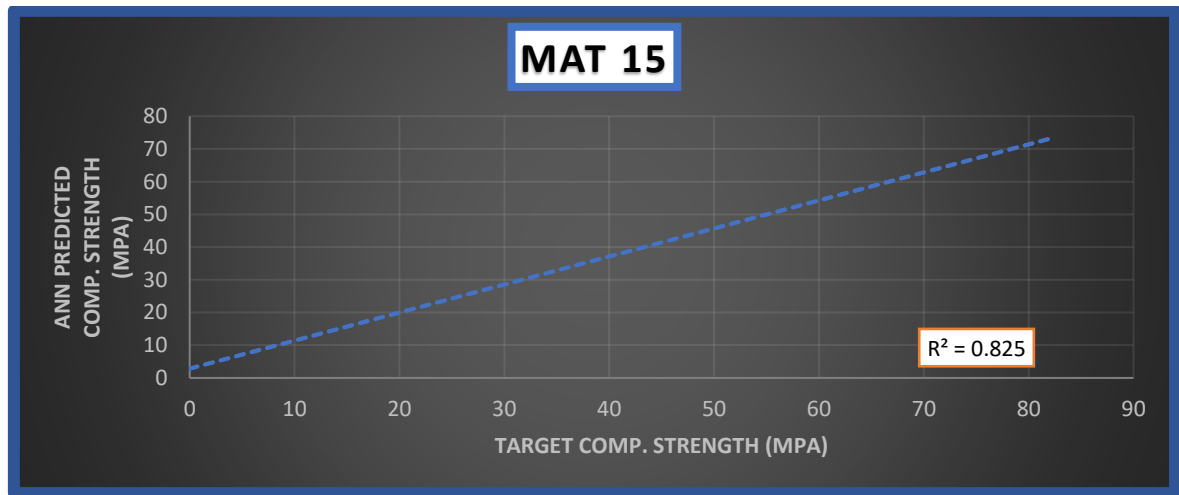


Figure 5: Target vs. ANN (15 neurons) (3 days) compressive strength

For Fig 4, 5 and 6, the compressive strength of 7 days is used for the prediction which has the MRA and ANN analysis respectively here it also shows that the ANN model is better for the prediction as its error limit is less and it will give a proper prediction.

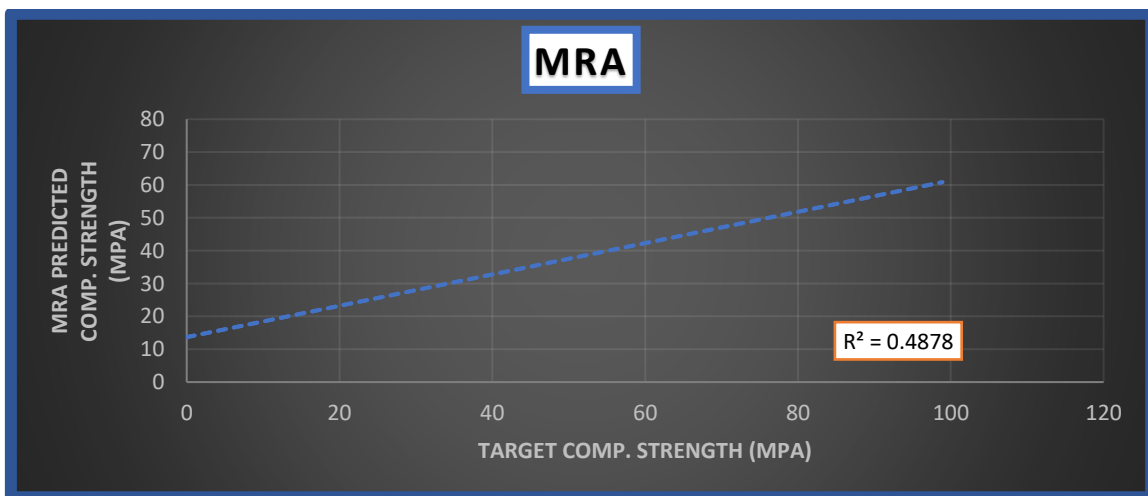


Figure 6: Target vs. MRA (7 days) compressive strength

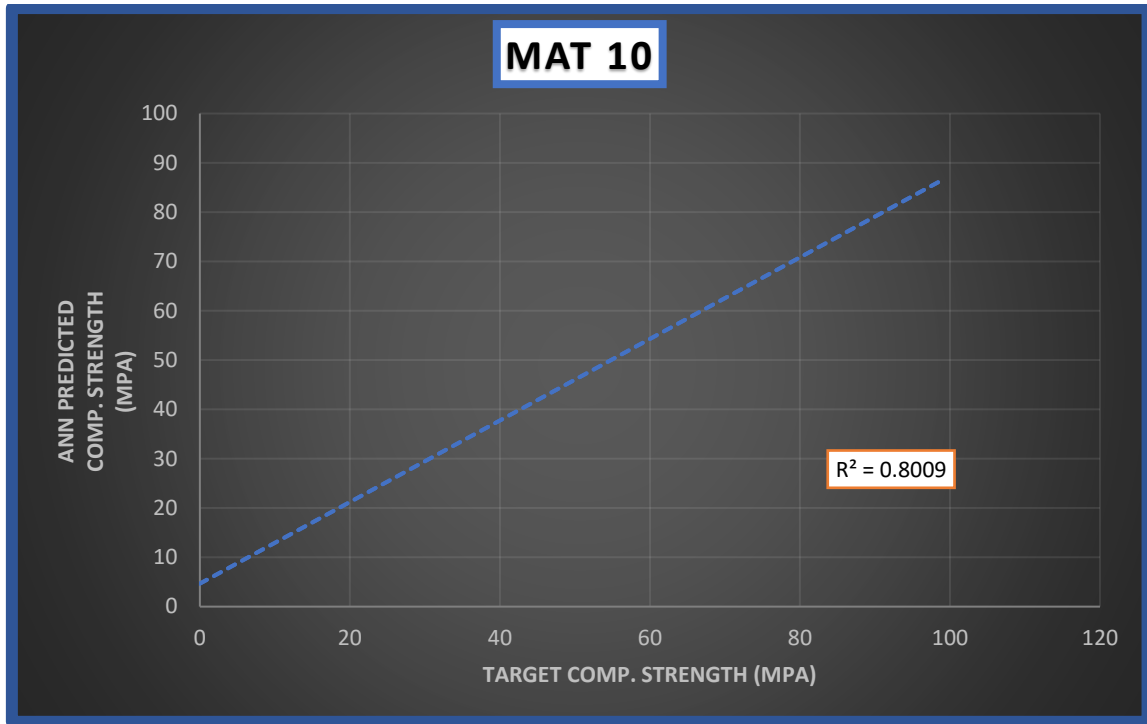


Figure 7: Target vs. ANN (10 Neurons) (7 days) compressive strength

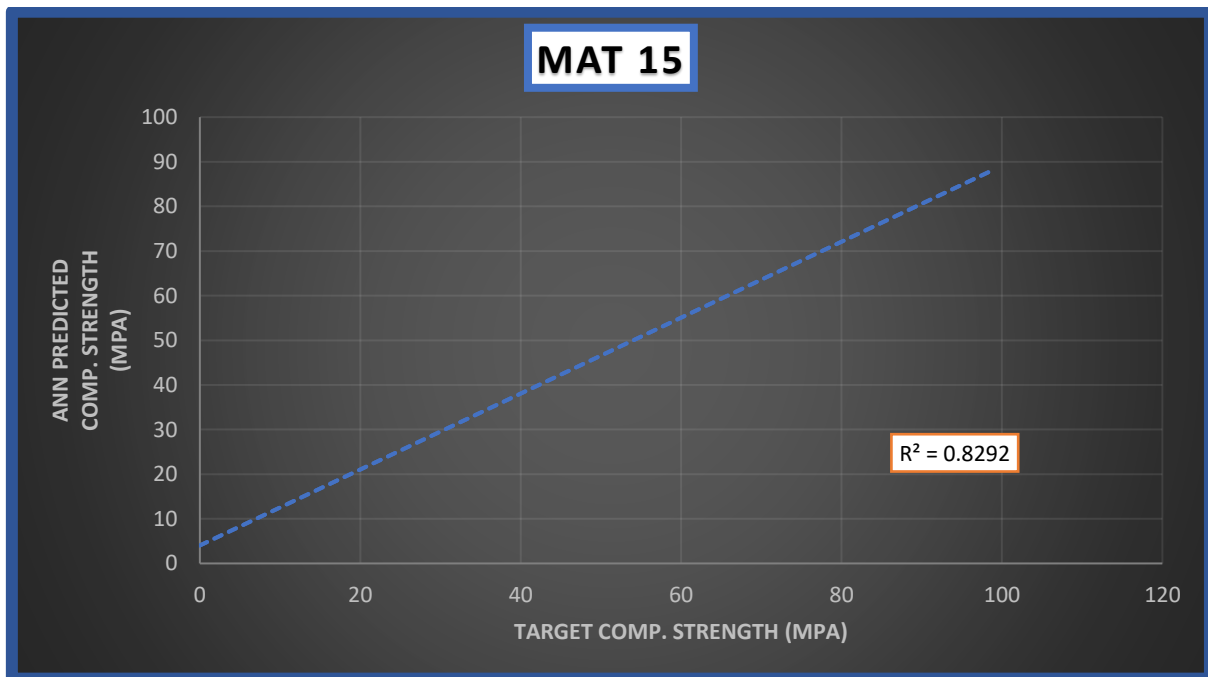


Figure 8: Target vs. ANN (15 Neurons) (7 days) compressive strength

For Fig. 7,8 and 9, the compressive strength of 14 days is used for the prediction with MRA and ANN model and it shows that the ANN has the R^2 value of 0.8188 for 10 neurons, 0.7948 for 15 neurons and for MRA has the R^2 value of 0.5433 so the ANN model is the best for prediction.

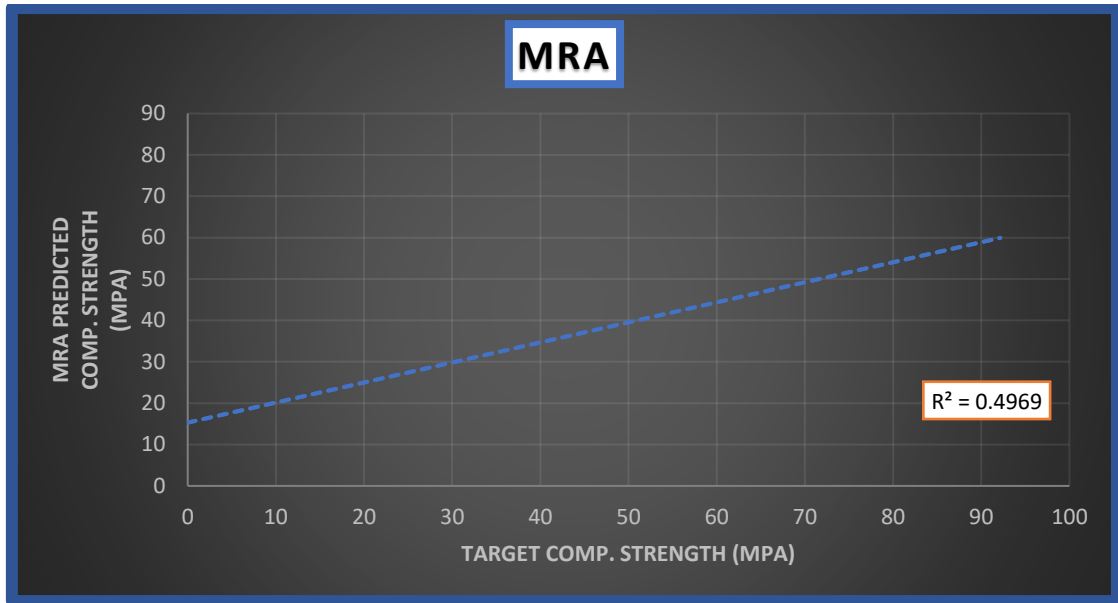


Figure 9: Target vs. MRA (14 days) compressive strength

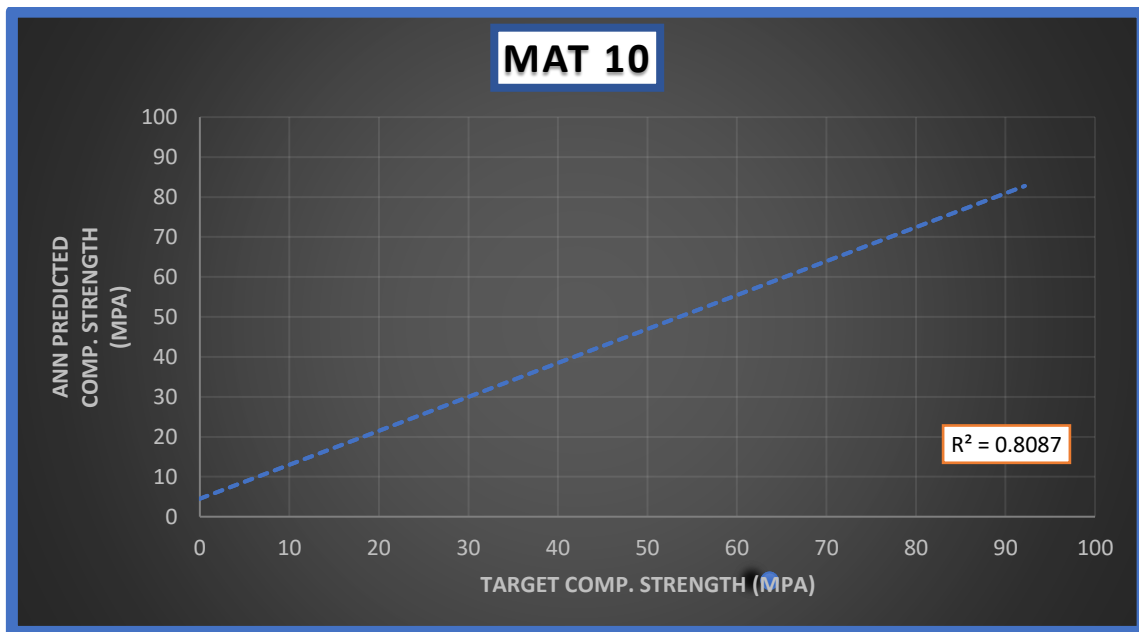


Figure 10: Target vs. ANN (10 Neurons) (14 days) compressive strength

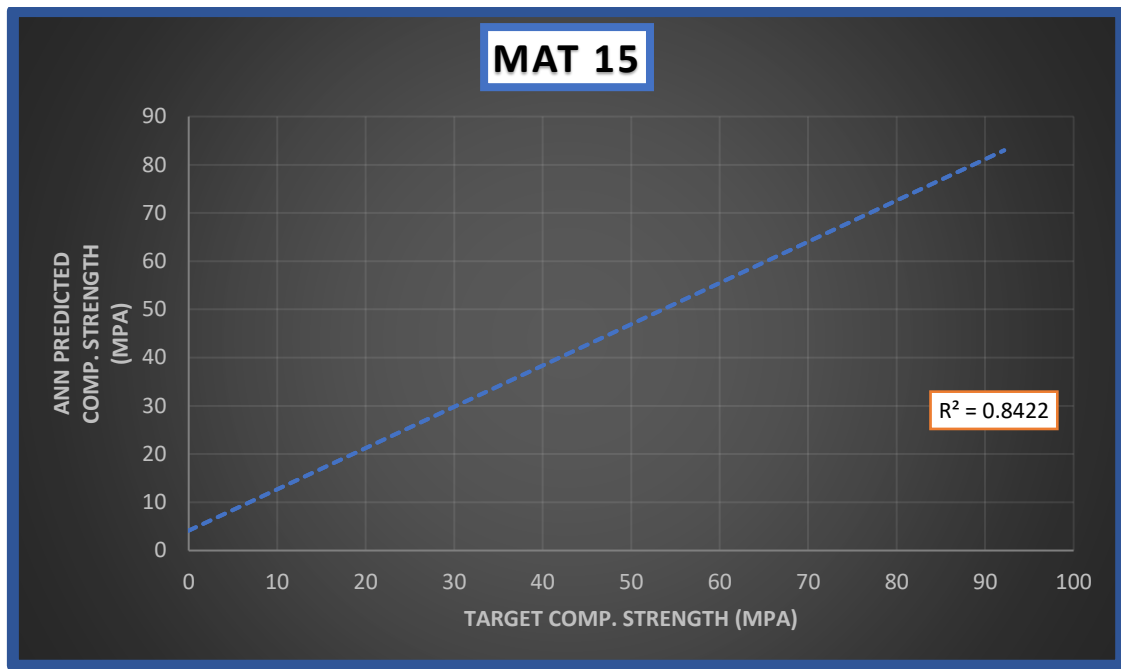


Figure 11: Target vs. ANN (15 Neurons) (14 days) compressive strength

For Fig. 10,11 and 12, compressive strength of 28 days is used for the prediction which has the MRA and ANN analysis respectively here it also shows that the ANN model is better for the prediction as its error limit is less and it will give a proper prediction.

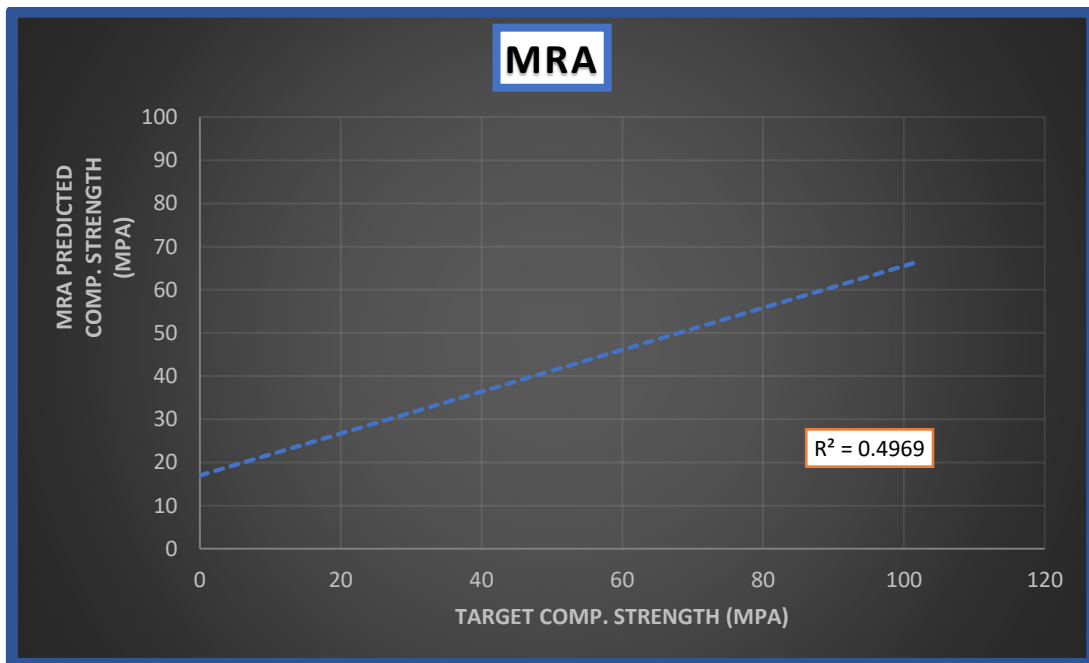


Figure 12: Target vs. MRA (28 days) compressive strength

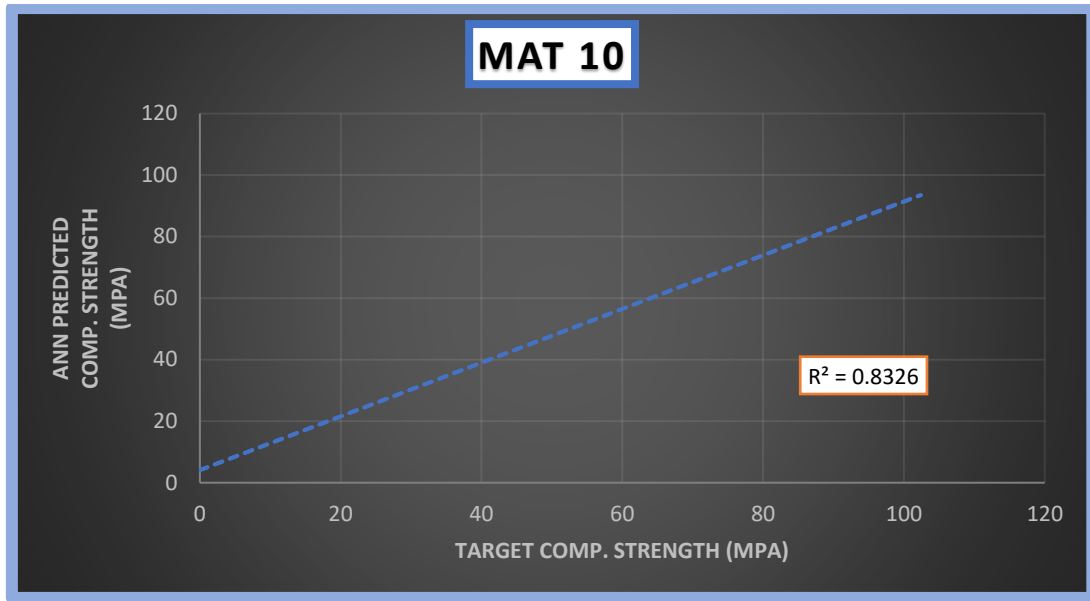


Figure 13: Target vs. ANN (10 Neurons) (28 days) compressive strength

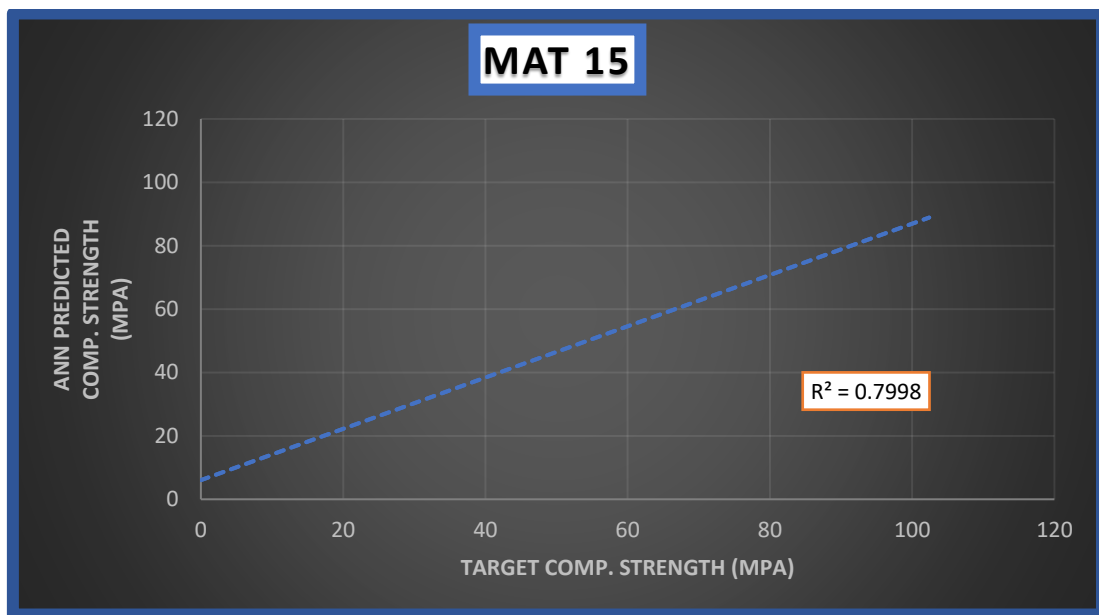


Figure 24: Target vs. ANN (15 Neurons) (28 days) compressive strength

For Fig. 13,14 and 15, density of concrete is used for the prediction which has the MRA and ANN analysis respectively

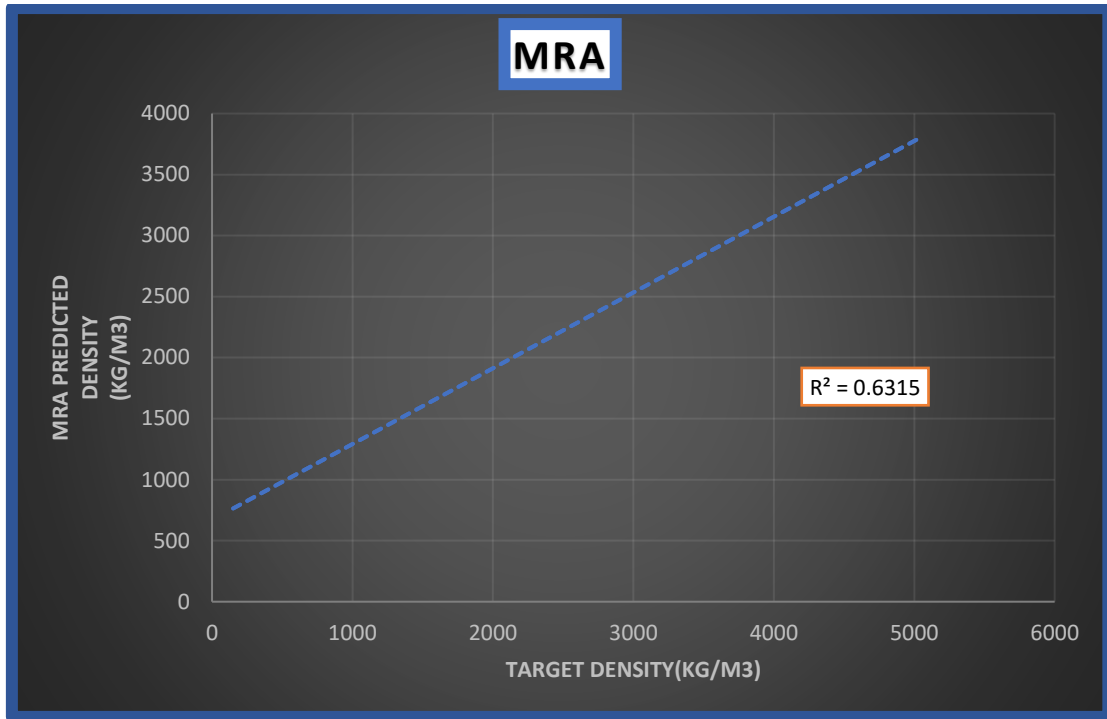


Figure 35: Target vs. MRA Density

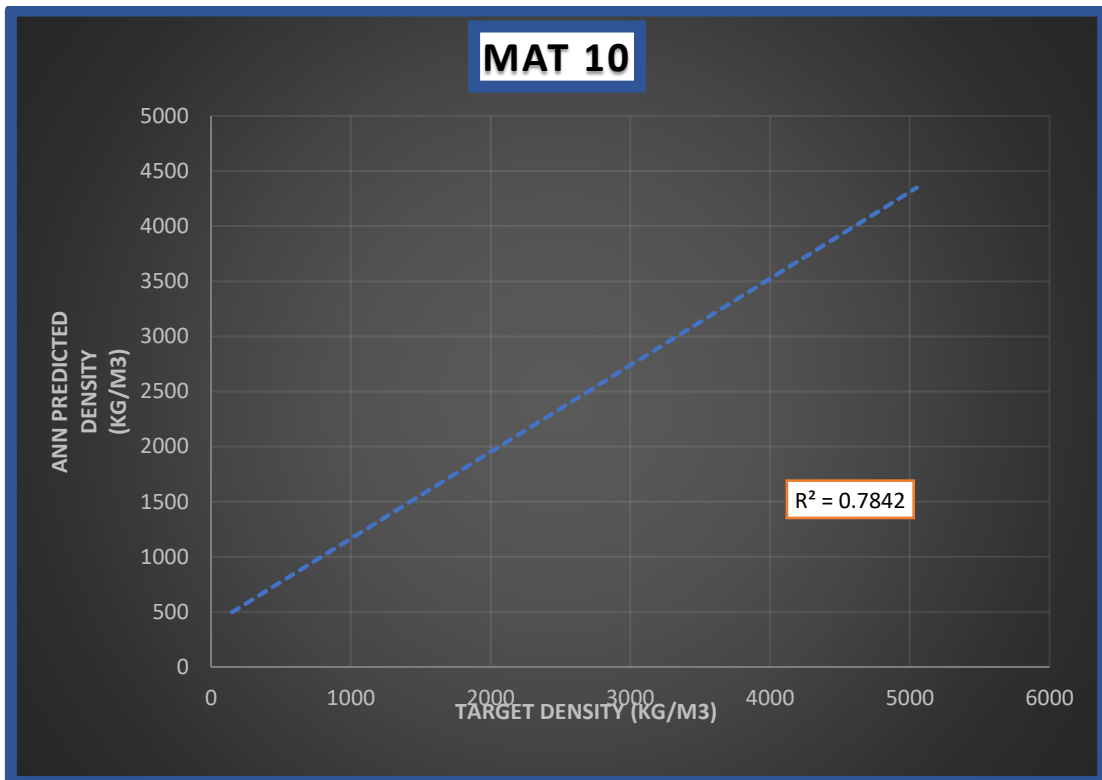


Figure 46: Target vs. ANN (10 Neurons) Density

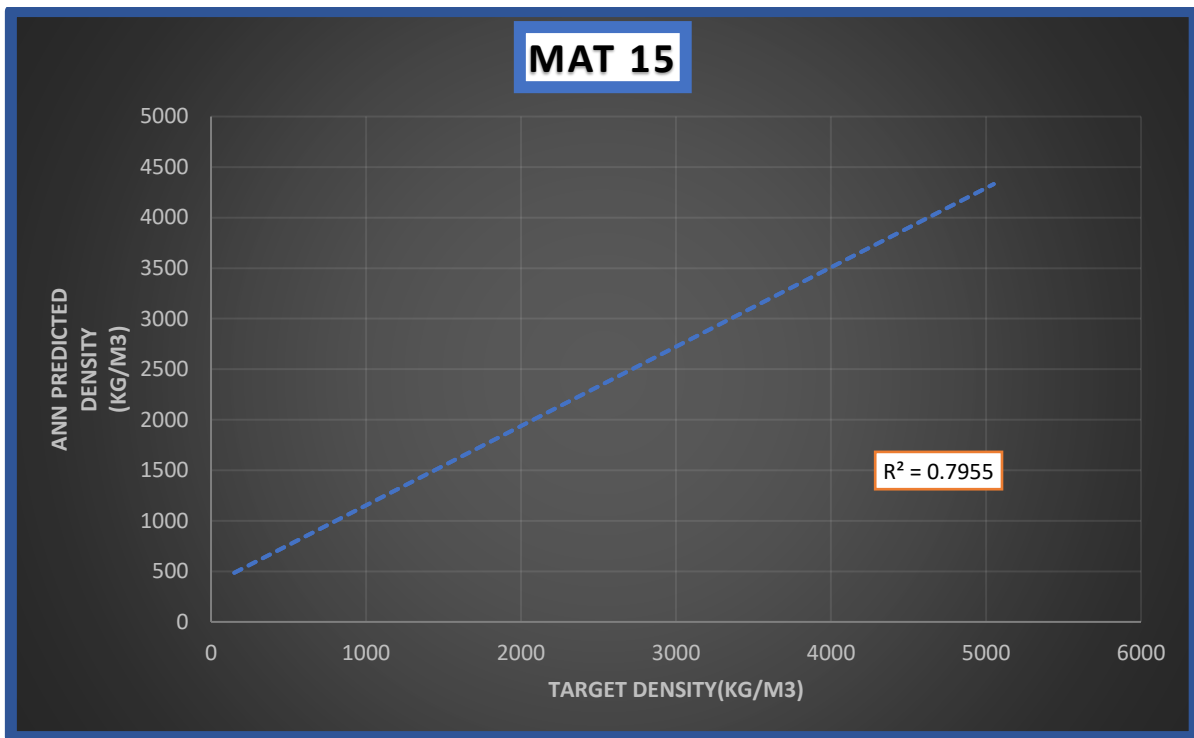


Figure 57: Target vs. ANN (15 Neurons) Density

For Fig. 16,17 and 18, Split Tensile strength is used for the prediction which has the MRA and ANN analysis respectively.

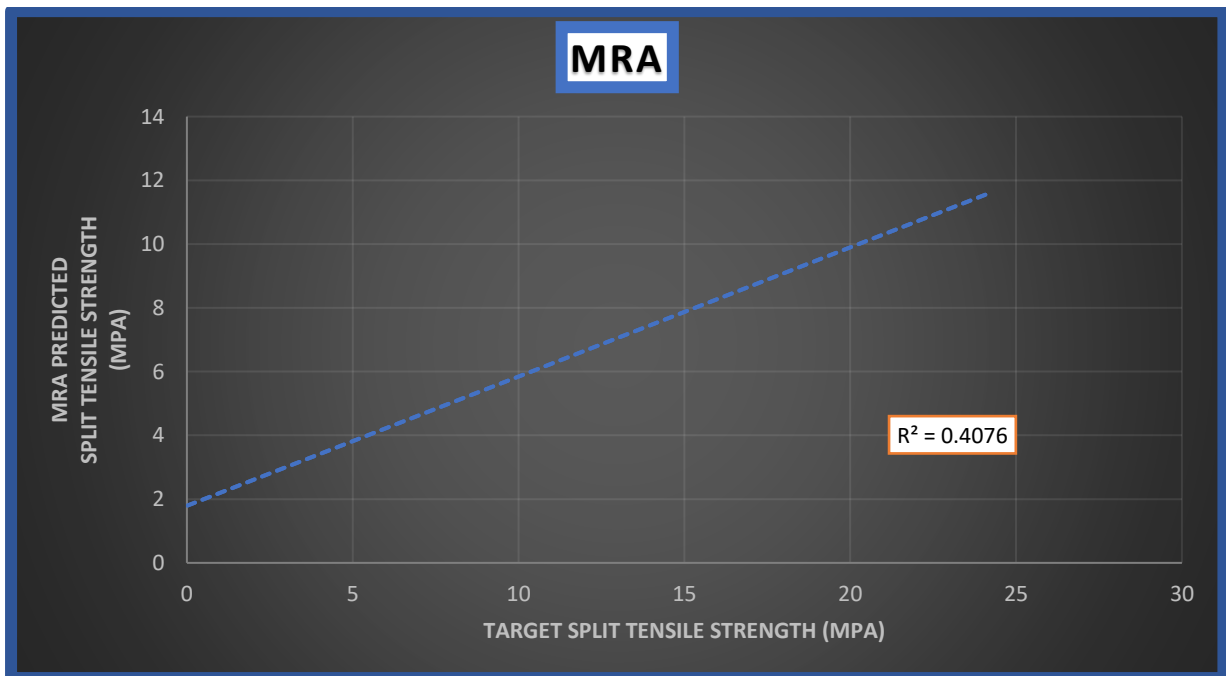


Figure 68: Target vs. MRA (28 days) Split Tensile Strength

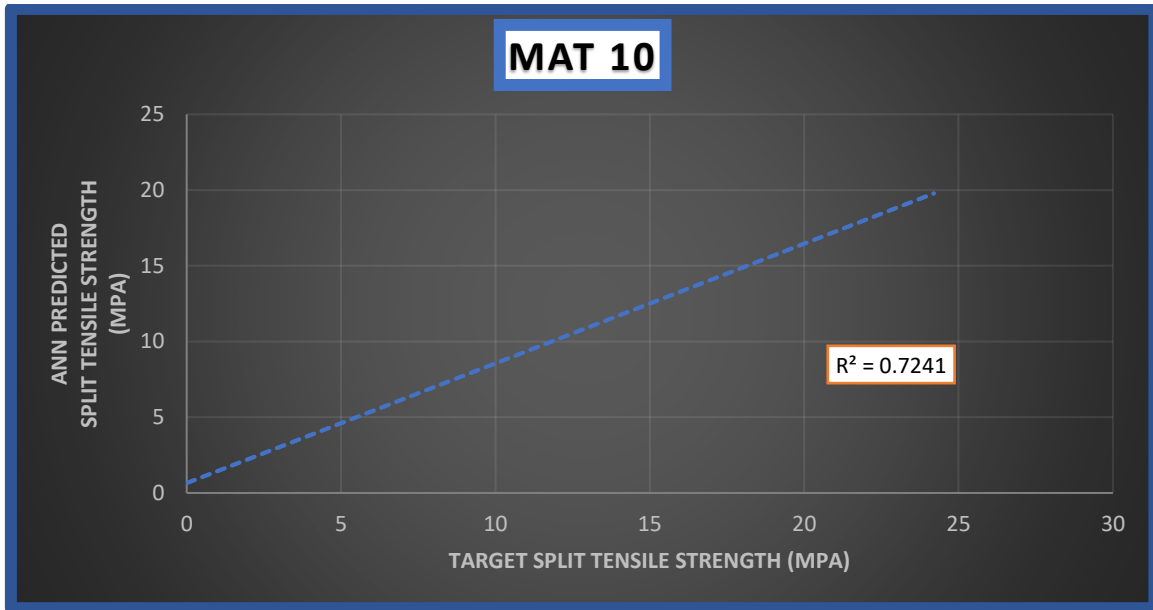


Figure 79: Target vs. ANN (10 Neurons) Split Tensile Strength

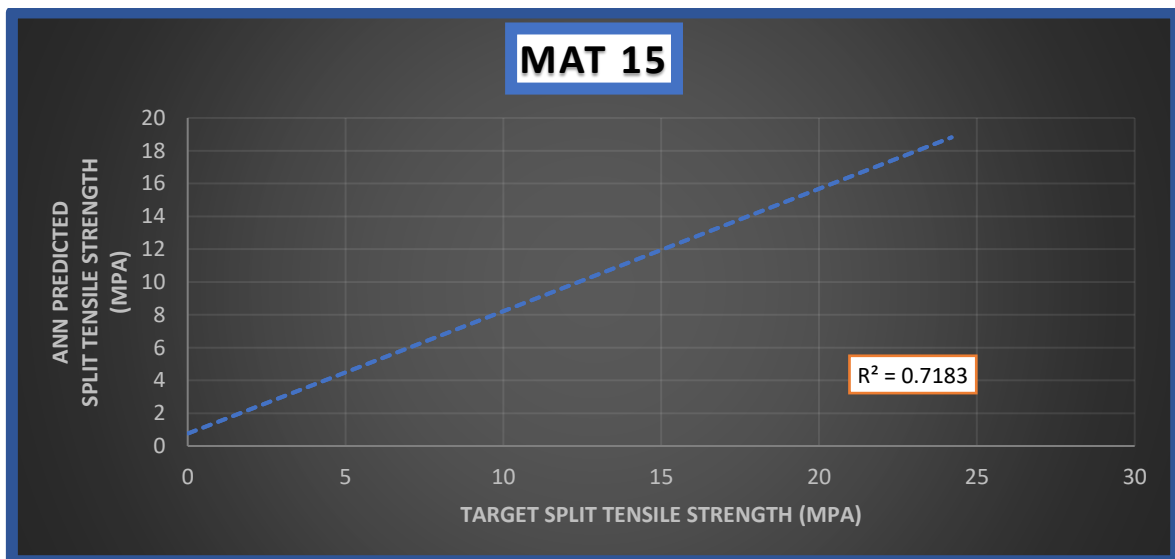


Figure 20: Target vs. ANN (15 Neurons) Split Tensile Strength

4. Conclusion:

This study portraits a MRA & ANN-based prediction model for the mechanical, split tensile strength & density of LWAC. The whole prediction is given by R^2 value. This study probes the doability of modelling a predictive analysis through earlier study data, transfiguring the unstructured factors to possible structured parameters & using those in creating the MRA model & ANN model. Also, the efficacy of these models is trailed using statistical tools such as R^2 and RMSE. The result shows that

1. For 3 days compressive strength, ANN model (15neurons) gives the maximum R^2 value of 0.8675 when compared to ANN (10neurons) & MRA has a R^2 value 0.4753 with RMSE of 7.9.
2. For 7 days compressive strength, ANN model (15neurons) gives the maximum R^2 value of 0.82929 when compared to ANN (10neurons) & MRA has a R^2 value 0.4878with RMSE of 9.958.

3. For 14 days compressive strength, ANN model (15neurons) gives the maximum R^2 value of 0.8422 when compared to ANN (10neurons) & MRA has a R^2 value 0.4969 with RMSE of 10.715.
4. For 28 days compressive strength, ANN model (15 neurons) gives the maximum R^2 value of 0.8498 when compared to ANN (10 neurons) & MRA has a R^2 value 0.4969 with RMSE of 11.877.
5. For split tensile strength, ANN model (15 neurons) gives the maximum R^2 value of 0.7383 when compared to ANN (10 neurons) & MRA has a R^2 value 0.4076 with RMSE of 1.276.
6. For density, ANN model (15 neurons) gives the maximum R^2 value of 0.7955 when compared to ANN (10 neurons) & MRA has a R^2 value 0.6315with RMSE of 250.599.

References:

1. Ke, Y.; Ortola, S.; Beaucour, A.L.; Demotte, H. Identification of microstructural characteristics in lightweight aggregate concretes by micromechanical modelling including the interfacial transition zone (ITZ). *Cem. Concr. Res.* 2010, 40, 1590–1600. [CrossRef]
2. Rossignolo, J.A.; Agnesini, M.V.C.; Morais, J.A. Properties of high-performance LWAC for precast structures with Brazilian lightweight aggregates. *Cem. Concr. Compos.* 2003, 25, 77–82. [CrossRef]
3. Elsharief, A.; Cohen, M.D.; Olek, J. Influence of lightweight aggregate on the microstructure and durability of mortar. *Cem. Concr. Res.* 2005, 35, 1368–1376. [CrossRef]
4. Nguyen, L.H.; Beaucour, A.L.; Ortola, S.; Noumowé, A. Influence of the volume fraction and the nature of fine lightweight aggregates on the thermal and mechanical properties of structural concrete. *Constr. Build. Mater.* 2014, 51, 121–132. [CrossRef]
5. Yoon, J.Y.; Lee, J.Y.; Kim, J.H. Use of raw-state bottom ash for aggregates in construction materials. *J. Mater. Cycles Waste Manag.* 2019, 21, 838–849. [CrossRef]
6. ASTM C330/C330M-17a. Standard Specification for Lightweight Aggregates for Structural Concrete; ASTM International: West Conshohocken, PA, USA, 2017.
7. Guide for Structural Lightweight-Aggregate Concrete; ACI 213R-14; American Concrete Institute: Farmington Hills, MI, USA, 2014
8. Kim, Y.J.; Choi, Y.W.; Lachemann, M. Characteristics of self-consolidating concrete using two types of lightweight coarse aggregates. *Constr. Build. Mater.* 2010, 24, 11–16. [CrossRef]
9. Bogas, J.A.; Gomes, A.; Pereira, M.F.C. Self-compacting lightweight concrete produced with expanded clay aggregate. *Constr. Build. Mater.* 2012, 35, 1013–1022. [CrossRef]
10. Kockal, N.U.; Ozturan, T. Strength and elastic properties of structural lightweight concretes. *Mater. Des.* 2011, 32, 2396–2403. [CrossRef]
11. Kanadasan, J.; Razak, H.A. Mix design for self-compacting palm oil clinker concrete based on particle packing. *Mater. Des.* 2014, 56, 9–19. [CrossRef]
12. Nepomuceno, M.C.S.; Pereira-de-Oliveira, L.A.; Pereira, S.F. Mix design of structural lightweight self-compacting concrete incorporating coarse lightweight expanded clay aggregates. *Constr. Build.*

- Mater. 2018, 166, 373–385. [CrossRef]
13. Lippmann, R. An introduction to computing with neural nets. *IEEE ASSP Mag.* 1987, 4, 4–22. [CrossRef]
 14. Ni, H.G.; Wang, J.Z. Prediction of compressive strength of concrete by neural networks. *Cem. Concr. Res.* 2000, 30, 1245–1250. [CrossRef]
 15. Belalia Douma, O.; Boukhatem, B.; Ghrici, M.; Tagnit-Hamou, A. Prediction of properties of self-compacting concrete containing fly ash using artificial neural network. *Neural Comput. Appl.* 2017, 28, 707–718. [CrossRef]
 16. Öztaş, A.; Pala, M.; Özbay, E.; Kanca, E.; Çağlar, N.; Bhatti, M.A. Predicting the compressive strength and slump of high strength concrete using neural network. *Constr. Build. Mater.* 2006, 20, 769–775. [CrossRef]
 17. Alshihri, M.M.; Azmy, A.M.; El-Bisy, M.S. Neural networks for predicting compressive strength of structural light weight concrete. *Constr. Build. Mater.* 2009, 23, 2214–2219. [CrossRef]
 18. Tavakkol, S.; Alapour, F.; Kazemian, A.; Hasaninejad, A.; Ghanbari, A.; Ramezani-pour, A.A. Prediction of lightweight concrete strength by categorized regression, MLR and ANN. *Comput. Concr.* 2013, 12, 151–167. [CrossRef]
 19. Davraz, M.; Kiliçarslan, S.; Ceylan, H. Predicting the Poisson Ratio of Lightweight Concretes using Artificial Neural Network. *Acta Phys. Pol. A* 2015, 128, B-184–B-187. [CrossRef]
 20. Tenza-Abril, A.J.; Villacampa, Y.; Solak, A.M.; Baeza-Brotons, F. Prediction and sensitivity analysis of compressive strength in segregated lightweight concrete based on artificial neural network using ultrasonic pulse velocity. *Constr. Build. Mater.* 2018, 189, 1173–1183. [CrossRef]
 21. Kalman Šipoš, T.; Miličević, I.; Siddique, R. Model for mix design of brick aggregate concrete based on neural network modelling. *Constr. Build. Mater.* 2017, 148, 757–769. [CrossRef]
 22. Demir, F. Prediction of elastic modulus of normal and high strength concrete by artificial neural networks. *Constr. Build. Mater.* 2008, 22, 1428–1435. [CrossRef]
 23. Atici, U. Prediction of the strength of mineral admixture concrete using multivariable regression analysis and an artificial neural network. *Expert Syst. Appl.* 2011, 38, 9609–9618. [CrossRef]
Materials 2019, 12, 2678 20 of 21
 24. Bal, L.; Buyle-Bodin, F. Artificial neural network for predicting drying shrinkage of concrete. *Constr. Build. Mater.* 2013, 38, 248–254. [CrossRef]
 25. Hossain, K.M.A.; Anwar, M.S.; Samani, S.G. Regression and artificial neural network models for strength properties of engineered cementitious composites. *Neural Comput. Appl.* 2018, 29, 631–645. [CrossRef]

26. Khademi, F.; Jamal, S.M.; Deshpande, N.; Londhe, S. Predicting strength of recycled aggregate concrete using Artificial Neural Network, Adaptive Neuro-Fuzzy Inference System and Multiple Linear Regression. *Int. J. Sustain. Built Environ.* 2016, 5, 355–369. [CrossRef]
27. Alengaram, U.J.; Mahmud, H.; Jumaat, M.Z. Enhancement and prediction of modulus of elasticity of palm kernel shell concrete. *Mater. Des.* 2011, 32, 2143–2148. [CrossRef]
28. Wee, T.H.; Chin, M.S.; Mansur, M.A. Stress-Strain Relationship of High-Strength Concrete in Compression. *J. Mater. Civ. Eng.* 1996, 8, 70–76. [CrossRef]
29. Guneyisi, E.; Gesoglu, M.; Booya, E. Fresh properties of self-compacting cold bonded fly ash lightweight aggregate concrete with different mineral admixtures. *Mater. Struct.* 2012, 45, 1849–1859. [CrossRef]
30. Bogas, J.A.; Gomes, A. A simple mix design method for structural lightweight aggregate concrete. *Mater. Struct.* 2013, 46, 1919–1932. [CrossRef]